Materials Science & Engineering B 236–237 (2018) 147–152

Contents lists available at ScienceDirect

Materials Science & Engineering B

journal homepage: www.elsevier.com/locate/mseb

General rules of the sub-band gaps in group-IV (Si, Ge, and Sn)-doped I-III-VI_2-type chalcopyrite compounds for intermediate band solar cell: A first-principles study

Dan Huang[a,c], Jing-Wen Jiang[a], Jin Guo[a,c], Yu-Jun Zhao[b,*], Rongzhen Chen[d], Clas Persson[d,e,*]

[a] Guangxi Key Laboratory for Relativistic Astrophysics, Guangxi Colleges and Universities Key Laboratory of Novel Energy Materials and Related Technology, Guangxi Novel Battery Materials Research Center of Engineering Technology, Guangxi Key Laboratory of Processing for Non-Ferrous Metallic and Featured Materials, School of Physical Science and Technology, Guangxi University, Nanning 530004, China

[b] Department of Physics and Key laboratory of Advanced Energy Storage Materials of Guangdong Province, South China University of Technology, Guangzhou 510640, China

[c] Guangxi Collaborative Innovation Center of Structure and Property for New Energy and Materials, School of Material Science and Engineering, Guilin University of Electronic Technology, Guilin, China

[d] Department of Materials Science and Engineering, Royal Institute of Technology, SE-100 44 Stockholm, Sweden

[e] Centre for Materials Science and Nanotechnology and Department of Physics, University of Oslo, PO Box 1048 Blindern, NO-0316 Oslo, Norway

ARTICLE INFO

Keywords:
Intermediate band solar cell
Chalcopyrite compound
First-principles calculation
Doping

ABSTRACT

In this work, we have investigated Si, Ge and Sn doped at III-site(Ga or Al) in $CuGaSe_2$, $CuAlSe_2$, $AgGaSe_2$, and $AgAlSe_2$ as the candidates for intermediate band solar cell (IBSC), and demonstrated that the absolute energy levels of the intermediate band from a given group IV dopant in various Se-based chalcopyrite hosts do not show remarkable changes. This is resulted from the fact that the intermediate band originates from the same anti-bonding state of IV-s and Se-p states. The intermediate bands sequence of $Ge^* < Sn^* < Si^*$ from the different dopants in the same chalcopyrite host is explained by a simple model based on the atomic orbital energy and bond interaction. Furthermore, Sn-doped $CuAlSe_2$ with the suitable main-gap and sub-gaps has been selected out as a potential candidate for IBSC, and alloying with isovalent cations to adjust to proper sub-band gaps has been demonstrated in Ge-doped $(Ag,Cu)AlSe_2$ and $Ag(Ga,Al)Se_2$.

1. Introduction

As an absorber for the solar cell, I-III-VI_2-type chalcopyrite compounds have been paid a lot of attention in the past decades [1,2]. Especially, the efficiency of the solar cell device based on $Cu(In,Ga)Se_2$ has reached to 22.6% on a laboratory scale [3], close to the maximum theoretical efficiency (31%) of the absorber with a single band gap (~1.5 eV) under one sun concentration [4]. To overcome the so-called SQ (Shockley and Queisser) limit [4], the idea based on inserting an intermediate band (IB) in the pristine band gap has been proposed by Luque and Martí in 1997 [5]. With the suitable band gap of the host and the ideal position of the IB, the maximum theoretical efficiency can promote to 46.8% under one sun concentration [5]. The requirements for the ideal width of the main band gap and two sub-band gaps to get the maximum under one sun concentration are 2.40, 1.48 and 0.92 eV [6,7], respectively. Providing that the two sub-band gaps are in the two intervals $1.30\ \text{eV} \le E_1 \le 1.65\ \text{eV}$ and $0.76\ \text{eV} \le E_2 \le 1.06\ \text{eV}$ [7], respectively, the intermediate band solar cell (IBSC) can also reach to a high efficiency.

Recently, chalcopyrite compounds with large band gap ($CuGaSe_2$ [8], $CuAlSe_2$ [9], $CuInS_2$ [10,11], $CuGaS_2$ [12–24], $CuAlS_2$ [25] etc.) have been studied as the hosts for IBSC. For the dopant, besides the transition metals like Ti [12], Cr [13], Fe [14] etc., the group-IV element Sn with delocalized 5*s* electrons has been suggested as the promising candidate to induce the IB in chalcopyrite compounds [15]. The same group elements Si and Ge [16] have rarely been reported as the dopants for IBSC experimentally. A half-filled IB and the increased absorption coefficient have been reported [17] in group-IV (C, Si, Ge, and Sn) doped at Ga site in $CuGaS_2$ by using the first-principles calculation based on the traditional LDA exchange–correlation functional.

* Corresponding authors at: Department of Physics and State Key Laboratory of Luminescent Materials and Devices, South China University of Technology, Guangzhou 510640, China (Y.J. Zhao) and Centre for Materials Science and Nanotechnology and Department of Physics, University of Oslo, PO Box 1048 Blindern, NO-0316 Oslo, Norway (C. Persson).

E-mail addresses: zhaoyj@scut.edu.cn (Y.-J. Zhao), clas.persson@fys.uio.no (C. Persson).

https://doi.org/10.1016/j.mseb.2018.11.006
Received 18 September 2017; Received in revised form 18 September 2018; Accepted 17 November 2018
Available online 28 November 2018
0921-5107/ © 2018 Elsevier B.V. All rights reserved.

However, it is difficult to clearly describe the physical mechanism behind the IB positions induced by the different dopants because the traditional LDA strongly underestimates the band gap up to 50% and then get the sub-band gap inaccurately.

Except our recent theoretical study on $AgAlTe_2$ [26], earlier studies on the host of IBSC from chalcopyrite compounds mainly focused on Cu-based compounds. With the alteration on the cations in I-III-VI_2 chalcopyrite compounds (i.e. I = Cu and Ag; III = Al, Ga, and In), the compounds exhibit different gap energies, and then also different sub-band gaps in case of the insertion of IB. Moreover, these chalcopyrite compounds provide the advantages of a controllable band gap and band edge positions by alloying different isovalent components [27]. For examples, the multi-element alloy (Ag,Cu)(In,Ga)Se_2 has been studied as the absorber for the solar cell [28–30]. The theoretical efficiency of IBSC is directly related to the values of band gap and sub-band gaps of the absorber. Therefore, it is important to unravel the physical mechanism on the positions of the IBs with the cation alteration in I-III-VI_2 chalcopyrite compounds, which can also help us to find the appreciate isovalent components to adjust the band gap as well as the sub-band gaps.

In this paper, group IV elements Si, Ge and Sn doping at the III-site (i.e. Al or Ga) in four kinds of Se-based chalcopyrite compounds, i.e. $CuGaSe_2$, $CuAlSe_2$, $AgAlSe_2$, $AgGaSe_2$, have been investigated by the HSE hybrid functional calculations. It is found that the absolute energy levels of the IBs from the same dopant in different chalcopyrite hosts do not show remarkable changes, which is explained according to the formation mechanism of the IBs. Our results reveal that Sn-doped $CuAlSe_2$ holds reasonable sub-band gaps and has the potential to realize high efficiency. In addition, it is demonstrated that isovalent cation alloying is a feasible approach to adjust the two sub-band gaps to a desired width for ideal absorbers of IBSC.

2. Computational details

Our first-principles calculations have been performed by using VASP package with plane wave basis to describe the valence states [31]. The projector augmented wave (PAW) method [32] has been used to describe the interactions between the valence electrons and the frozen core. The cutoff energy for the plane wave basis is set as 400 eV for all calculations. In order to get a reasonable band gap, the HSE (i.e. Heyd, Scuseria and Ernzerhof) hybrid exchange–correlation functional has been adopted [33]. To minimize the band gap deviation from the experimental values [34] (see Table 1), the amount of Hartree-Fock exchange is adjusted to $\alpha = 0.30$ as the screening parameter $\omega = 0.20$ bohr^{-1} is kept. As listed in Table 1, the calculated lattice parameters are still in good agreement with the experimental values [34] by using our selected exchange–correlation functional. For the calculations on Si, Ge and Sn substituting at III-site (i.e. Al or Ga) in these chalcopyrite compounds, a $2 \times 2 \times 1$ supercell (64 atoms) has been adopted. A Γ-centered $2 \times 2 \times 2$ **k**-mesh [35] has been used for the lattice parameter relaxation and then a denser $3 \times 3 \times 3$ **k**-mesh has been used for the electronic structure calculations. For the band offset calculations on the four pure chalcopyrite compounds, the Γ-centered $4 \times 4 \times 1$ mesh is used for the eight unit cell layers A and B superlattice changing along the [0 0 1] -direction (64 atoms). The details for the band offset calculations are described in our previous paper [36]. For the optical property calculations, the imaginary part ε_2 of the dielectric function is calculated from the joint DOS and the optical momentum matrix elements between the occupied and unoccupied wave functions. The real part ε_1 of the dielectric function is obtained from the Kramers-Kronig relationship. The interband absorption is summed over all direct VB (valence band) to CB (conduction band) transitions. Owing to the half-filled property of the IBs and then the metallic characteristics, the intraband transition is accounted for by employing an empirical Drude term [37].

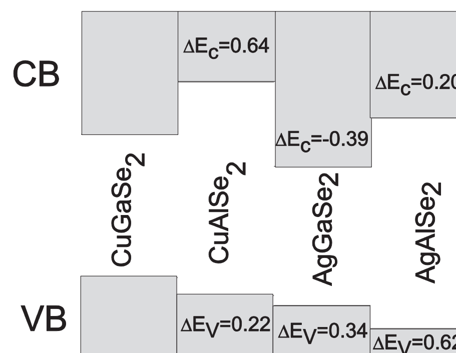

Fig. 1. The band offsets among $CuGaSe_2$, $CuAlSe_2$, $AgGaSe_2$ and $AgAlSe_2$. The VBM and CBM of $CuGaSe_2$ are set as the reference. The values of VB and CB offset of the other chalcopyrite compounds with respect to $CuGaSe_2$ are presented.

3. Results and discussion

3.1. The band offsets among $CuGaSe_2$, $CuAlSe_2$, $AgGaSe_2$ and $AgAlSe_2$

Fig. 1 shows the band offsets among the four kinds of chalcopyrite compounds, i.e. $CuGaSe_2$, $CuAlSe_2$, $AgGaSe_2$ and $AgAlSe_2$. The values on the VB offsets and CB offsets of the other chalcopyrite compounds with respect to $CuGaSe_2$ are also presented in Fig. 1. From the former study [38] and as shown in Fig. 2, we understand that the valence band maximum (VBM) comes from the antibonding state of group-I (i.e. Cu or Ag) *d* state and Se-4*p* state and the conduction band minimum (CBM) originates from the antibonding state of III(i.e. Ga or Al)-s state and Se-4p state. Since the Cu-Se bond has a shorter bond length than the Ag-Se bond, and Cu-3d state has a higher orbital energy than Ag-4d state, $CuAlSe_2$ and $CuGaSe_2$ are expected to have energetically higher VBMs than those of $AgAlSe_2$ and $AgGaSe_2$ [39]. Similarly, owing to that the Al-Se bond has a shorter bond length than the Ga-Se bond and the Al-3s state has a higher orbital energy than the Ga-4s state, $CuAlSe_2$ and $AgAlSe_2$ have higher CBMs than those of $CuGaSe_2$ and $AgGaSe_2$. Therefore, by alloying Cu or Al, the chalcopyrite compounds containing Ag or Ga can lift up the VBM or CBM, respectively. Our HSE calculated values on the band offsets are similar to the results from former GGA + U calculations [39], as a result of the fact that the band offset is a comparative value and one can get similar results by using different

Table 1
The lattice parameters *a* and *c*, the anion displacement parameter *u* and the band gap (BG) from our calculations and experiments [34]. The calculated BG deviations from experiments are also listed.

	Calculations				Experiments				
Species	*a*(Å)	*c*(Å)	*u*	*BG*(eV)	*a*(Å)	*c*(Å)	*u*	*BG*(eV)	*BG* Deviation
$CuGaSe_2$	5.621	11.002	0.253	1.75	5.614	11.022	0.259	1.68	4.2%
$CuAlSe_2$	5.617	10.995	0.257	2.60	5.606	10.901	0.257	2.65	−1.5%
$AgGaSe_2$	6.019	10.970	0.286	1.70	5.992	10.883	0.288	1.82	−6.6%
$AgAlSe_2$	5.994	10.964	0.289	2.57	5.956	10.750	0.270	2.55	0.8%

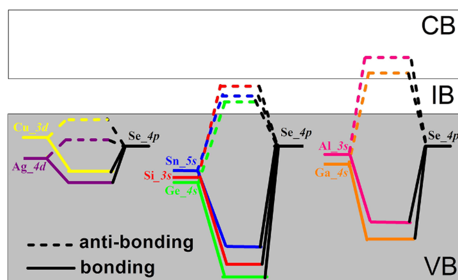

Fig. 2. Schematic diagram of the origns of VBM, IB and CBM in group-IV (Si, Ge, and Sn)-doped I-III-VI_2-type chalcopyrite compounds, which are from the antibonding states of I-d and VI-p states(VBM), IV-s and VI-p states(IB) and III-s and VI-p(CBM), repectively.

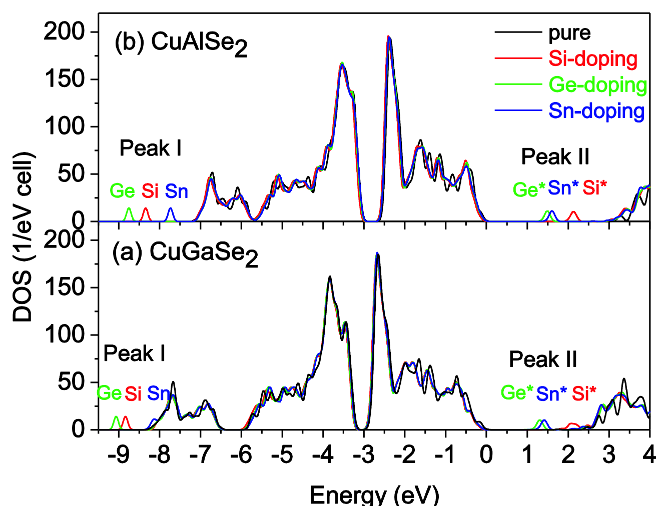

Fig. 3. The total density of states of pure and (Si, Ge, and Sn)-doped $CuGaSe_2$(a) and $CuAlSe_2$(b). The average potentials of host elements far away from the dopant are used to align the DOS. The energy is referenced to the VBM of $CuGaSe_2$ and $CuAlSe_2$, respectively.

exchange–correlation functionals.

3.2. Analyses of density of states and the sequence of IBs

Fig. 3a and b show the total density of states (DOS) of the pure and (Si, Ge, and Sn)-doped $CuAlSe_2$ and $CuGaSe_2$, respectively. After doping the group IV elements Si, Ge, and Sn at Ga or Al site, the pristine VB and CB in the DOS do not show a remarkable change. Two series of impurity peaks are presented in the DOS. The first one (Peak I) with the sequence of Ge < Si < Sn appears from around −9.5 to −7.5 eV. Another one (Peak II) appears in the band gap with the sequence of Ge* < Sn* < Si*, which is corresponding to the IBs. The Sn impurity peak at the low energy region (Peak I) in $CuGaSe_2$ merges with the energy band of host. Notably, the Si impurity peak (Peak II) in the band gap merges with CBM of $CuGaSe_2$, which results in the disappearance of IB in the band gap. The DOSs of $AgGaSe_2$ and $AgAlSe_2$ have similar characteristics with those of $CuGaSe_2$ and $CuAlSe_2$.

Fig. 4a and b show the partial density of states (PDOS) of Sn and Se bonding with the Sn in Sn-doped $CuAlSe_2$. One can observe that the IB in Sn-doped $CuAlSe_2$ (Peak II) is comprised of the Sn-s and Se-p states. The impurity Peak I in Sn-doped $CuAlSe_2$ also consists of Sn-s and Se-p states. The crystal orbital overlap populations (COOP) can help us to analyze the bonding interaction [40,41]. In Fig. 4c, the positive and negative values stand for bonding and antibonding interaction. Combining the PDOSs with COOP between Sn and Se in Sn-doped $CuAlSe_2$, we can explain that the Peak II arises from the antibonding state between Sn-s and Se-p states and the Peak I originates from the bonding

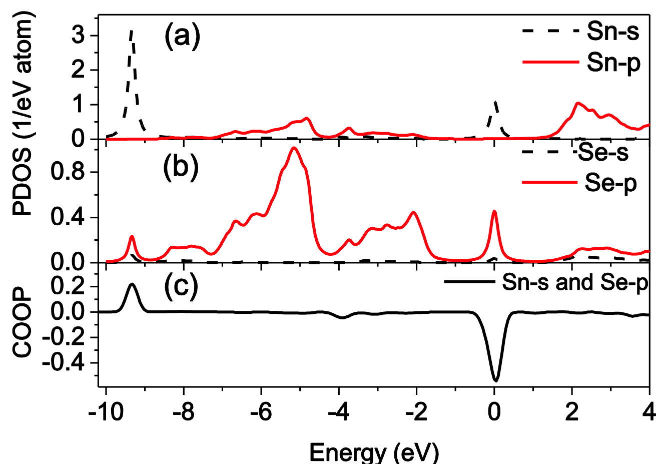

Fig. 4. The partial density of states of Sn(a) and Se(b) and the COOP(c) between Sn-s and Se-p in Sn-doped $CuAlSe_2$. The Fermi energy level is set to zero.

state between Sn-s and Se-p states. For other doped materials, the PDOS and COOP are similar with that in Sn-doped $CuAlSe_2$. In our former study, based on the orbital energy and bond length [26], we have explained the sequence of the IB in Si, Ge and Sn doped $AgAlTe_2$. As shown in the center part of Fig. 2, we found that the sequences of IBs of Ge* < Sn* < Si* in Si, Ge and Sn doped $CuGaSe_2$, $CuAlSe_2$, $AgGaSe_2$ and $AgAlSe_2$ are same to that in Si, Ge and Sn doped $AgAlTe_2$ from our former study[26]. Here, we can also use the same model to understand the sequences of IBs in our studied systems. Owing to the shortest bond length of Si-Se among the three bonds (i.e. Si-Se, Ge-Se and Sn-Se bonds), the antibonding state of Si-s and Se-p is pushed to the highest position. Owing to the lowest orbital energy[42] of Ge-s among the s orbital energy of three element (i.e. Si-3s, Ge-4s and Sn-5s), the bonding/antibonding states of Ge-s and Se-p still stay at the lowest positions. Then, we speculate that the sequence of IBs induced by Si, Ge and Sn doping in all I-III-VI_2-type chalcopyrite compounds should be the same as Ge* < Sn* < Si*.

3.3. The band offsets from the same hosts with different dopants

The band offsets among the pure compound and the systems with different dopants in the same host are calculated with the conventional approach, i.e., aligned by the average potentials of host elements far away from the dopant [43]. Fig. 5a and 5b present the band offsets in $CuAlSe_2$ and $AgAlSe_2$ with and without doping. The IBs induced by Si, Ge and Sn doping at Ga or Al site in these four kinds of chalcopyrite materials have the same sequence of Ge* < Sn* < Si*, which is in agreement with that in our former studied host material $AgAlTe_2$ [26]. According to above analyses on DOS and PDOS, we can explain the sequences of the IBs in these chalcopyrite materials after Si, Ge and Sn

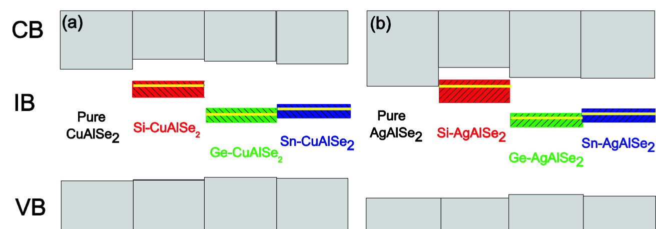

Fig. 5. The band offsets among the pure and (Si, Ge, and Sn)-doped $CuAlSe_2$(a) and the pure and (Si, Ge, and Sn)-doped $AgAlSe_2$(b). The VBM and CBM of $CuAlSe_2$ are set as the reference. The yellow lines stand for the calculated Fermi energy level of the (Si, Ge, and Sn)-doped supercells. (For interpretation of the references to colour in this figure legend, the reader is referred to the web version of this article.)

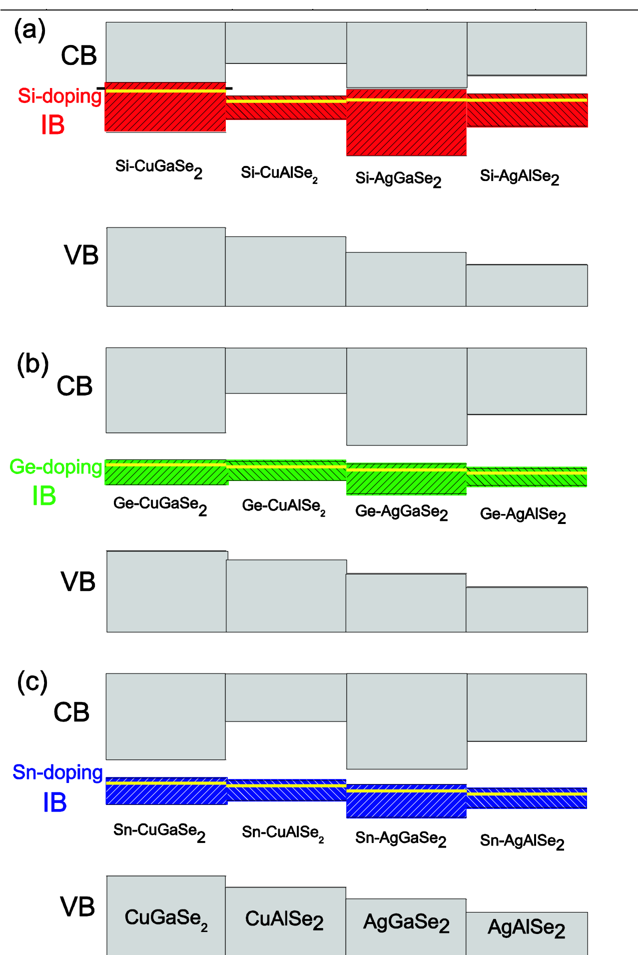

Fig. 6. The band offsets of Si-doped (a), Ge-doped (b) and Sn-doped (c) the four kinds of chalcopyrite compounds (i.e. $CuGaSe_2$, $CuAlSe_2$, $AgGaSe_2$ and $AgAlSe_2$). The yellow lines stand for the calculated Fermi energy level of the (Si, Ge, and Sn)-doped supercells. (For interpretation of the references to colour in this figure legend, the reader is referred to the web version of this article.)

doping, which supplies a simple clue to find a suitable dopant to adjust the IB position in the band gap.

3.4. The band offsets from different hosts with the same dopant

Combining with the band offsets in pure chalcopyrite compounds (Fig. 1) and the band offsets from the different dopants in the same host (Fig. 5), we can get the band offsets of different hosts with the same dopant. Fig. 6a–c show the band offsets of Si-doped, Ge-doped and Sn-doped the four kinds of chalcopyrite compounds, respectively. One observes that the absolute energy levels of the IBs in different hosts do not change significantly, which is related to that the IBs come from the same antibonding states of the same bonds (i.e. Si-Se, Ge-Se and Sn-Se bonds) although the cations of the hosts are different. Owing to the resonance between the IBs and the main band, the main band gap becomes larger than the pristine one, which is listed in Table 2. Although the main band gap becomes wider after doping, the sequence of VBM and CBM of the doped hosts also does not show a significant change with that of the pure compounds, which can also be explained by that compositions of the VBM and CBM do not change after Si, Ge and Sn doping at Ga or Al site. Since the Cu-based compounds have a higher VBM positions than corresponding Ag-based compounds (see Fig. 1), the sub-band gap I (i.e. from VBM to Fermi energy level) from the same dopant in Cu-based compounds is narrower than that in Ag-based analogues. For the same reason, the compounds containing Al have a higher CBM position than the compounds containing Ga (see Fig. 1), the sub-band gap II (i.e. from Fermi energy level to CBM) from the same dopant in Al-based compounds is wider than that in Ga-based analogues. From Fig. 6a, we notice that the IBs in Si-doped $CuGaSe_2$ and Si-doped $AgGaSe_2$ become wider than other IBs, which should be related to the stronger resonance between the IB by Si doping and the CBM from the compounds containing Ga. Owing to that Si doping produces a high IB and the compounds containing Ga have a low CBM, the IBs and CBM interact strongly and merge in Si doped $CuGaSe_2$ or almost merge of in Si doped $AgGaSe_2$ with each other, in which the two sub-band gaps almost disappear. Then, our results suggest that Si doping at Ga site in chalcopyrite compounds containing Ga (like $CuGaSe_2$ and $AgGaSe_2$) cannot induce an isolated IB in the band gap. In addition, the chalcopyrite compounds containing In have a lower CBM than that containing Ga [36], we can also draw the conclusion that Si-doping cannot induce an isolated IB in In-based compounds (for example, Si-doped $AgInS_2$).

3.5. The absorption coefficient and the width of the gaps

Fig. 7a–d show the absorption coefficients of the pure and Si, Ge and Sn doped $CuGaSe_2$ (a), $CuAlSe_2$ (b), $AgGaSe_2$ (c) and $AgAlSe_2$ (d), respectively. Comparing the absorption coefficients with and without the intraband correction, we have found that the coefficients blow 0.3 eV come from the intraband absorption which may heat up the device and is harmful for the IBSC. The absorption coefficients above 0.3 eV come from the interband absorption and are almost unchanged after the intraband correction. From the absorption coefficients of the pure and doped compounds, one observes that the absorption spectra of the compounds after doping have redshifted by the sub-band gap absorption. Since Si doping pushes the IB to a high energy position, the widths of sub-band gaps are less reasonable than these in Ge and Sn doping when considering these four chalcopyrite compounds as the host for IBSC. The abilities on visible light absorption of the compounds after Ge and Sn doping are stronger than that after Si-doping. The detailed widths of band gap, sub-gap and IB are listed in Table 2. To meet the requirements on the sub-band gaps to yield high theoretical efficiency, the widths of two sub-band gap need to locate in the two intervals $1.30\ eV \leq E_1 \leq 1.65\ eV$ and $0.76\ eV \leq E_2 \leq 1.06\ eV$ [7], respectively. We notice that only Sn doped $CuAlSe_2$ satisfies the two requirements at the same time and has the potential to realize the high efficiency. For Si-doped these four compounds, both requirements are not satisfied owing to the unreasonable IB positions. For other systems, they can meet one of the requirements and need to adjust the width of another sub-band gap. Since the VBM, CBM and IB come from the components of different bonding states (i.e. VBM from the antibonding state between I-d and Se-p, CBM from the antibonding state between III-s and Se-p and IB from the antibonding state IV-s and Se-p), alloying different isovalent cations in the chalcopyrite hosts may change the components at VBM and CBM and then adjust the band edge positions. From the band offsets of these four compounds in Fig. 1, we notice that Cu-alloying can lift up the energy position of VBM of Ag-based compounds and adjust the sub-band gap I from VBM to the Fermi energy level, and Al-alloying can lift up the CBM of the Ga-based compounds and adjust the sub-band gap II from the Fermi energy level to CBM. As a demonstration, we select Ge-doped $AgAlSe_2$ and Ge-doped $AgGaSe_2$ to adjust the sub-band gap I and sub-band gap II by Cu-alloying and Al-alloying, respectively. In the calculation supercells, the Cu or Al atoms have been distributed uniformly. From the width of the gaps in the compounds after Cu and Al alloying in Table 2, the VBM has been shifted up and the widths of sub-band gaps are close to the reasonable values in $(Ag_{12}Cu_4)(Ga_{15}Ge)Se_{32}$, as well as the CBM has been shifted up and the widths of sub-band gaps are moved to desired direction in $Ag_{16}(Ga_{11}Al_4Ge)Se_{32}$. Owing to that Cu-alloying (or Al-alloying) does not change the component of CBM (or VBM for Al-alloying), the widths of sub-band gap II (or sub-band gap I for Al-alloying) do not show a remarkable change with the VBM raising (or CBM raising for Al-alloying). Owing to the

Table 2
The widths of band gap, sub-band gap and IB (in eV) in the four kinds of chalcopyrite compounds $CuGaSe_2$, $CuAlSe_2$, $AgGaSe_2$ and $AgAlSe_2$ with and without doping.

System		Band gap	Sub-gap I (VBM − E_F)	Sub-gap II (E_F − CBM)	Width of IB
			[1.30, 1.65]	[0.76, 1.06]	
$CuGaSe_2$	pure	1.74			
	Si-doping	2.21	2.20	0.14	0.80
	Ge-doping	1.89	1.37	0.52	0.40
	Sn-doping	1.86	1.49	0.37	0.43
$CuAlSe_2$	pure	2.60			
	Si-doping	2.79	2.19	0.60	0.38
	Ge-doping	2.69	1.51	1.18	0.30
	Sn-doping	2.67	1.63	1.04	0.32
$AgGaSe_2$	pure	1.70			
	Si-doping	2.65	2.45	0.20	1.07
	Ge-doping	2.07	1.66	0.41	0.48
	$Ag_{16}(Ga_{11}Al_4Ge)Se_{32}$	2.15	1.67	0.48	0.42
	Sn-doping	2.08	1.74	0.34	0.53
$AgAlSe_2$	pure	2.57			
	Si-doping	3.02	2.63	0.39	0.51
	Ge-doping	2.76	1.82	0.94	0.27
	$(Ag_{12}Cu_4)(Ga_{15}Ge)Se_{32}$	2.64	1.67	0.97	0.25
	Sn-doping	2.75	1.90	0.85	0.30

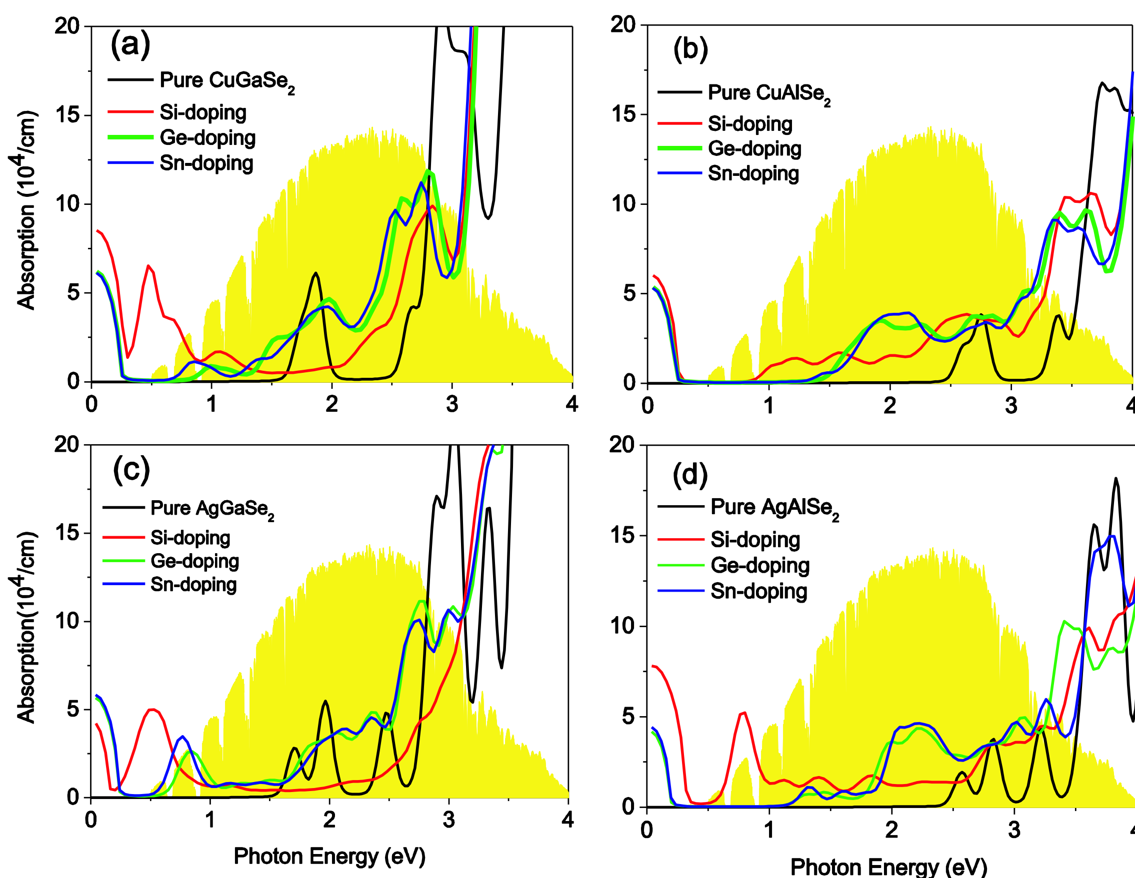

Fig. 7. The absorption coefficient of the four kinds of chalcopyrite compounds [$CuGaSe_2$(a), $CuAlSe_2$(b), $AgGaSe_2$(c) and $AgAlSe_2$(d)] with and without Si, Ge and Sn doping. The reference air-mass 1.5-solar spectral irradiance is plotted in yellow. (For interpretation of the references to colour in this figure legend, the reader is referred to the web version of this article.)

components of VBM, CBM and IB from separate contributions of different bonds in the chalcopyrite alloys, we expect that the compounds can be tuned into the ideal band gap for IBSC with careful isovalent cation alloying. Therefore, our results provide a suitable way to search the desired absorber in group-IV elements (Si, Ge and Sn) doped chalcopyrite compounds.

4. Conclusions

In summary, we have studied Si, Ge and Sn doped at the group III site in Se-based chalcopyrite, $CuGaSe_2$, $CuAlSe_2$, $AgAlSe_2$, and $AgGaSe_2$, as the potential absorbers for IBSC by the HSE hybrid functional calculations. Our results reveal that the IBs come from the Se-p dominated antibonding state of IV-s and Se-p, leading to the fact that the absolute

energy level of the IB is not sensitive to the alteration of the cations of the chalcopyrite compounds. The sequence of Ge* < Sn* < Si* on the IBs in the main band gaps of the chalcopyrite hosts is also explained by a simple model based on the atomic orbital energy and bond interaction. The Sn-doped $CuAlSe_2$ has the ideal sub-band gaps and can be regarded as a potential candidate for the absorber of IBSC. Alloying with isovalent cations is demonstrated to be able to adjust the sub-band gap, implying a potential and promising way to the search of desired absorbers of IBSC.

Acknowledgments

This work was financially supported by the National Natural Science Foundation of China (Grant Nos. 61664003, 51571065, and 11574088), Innovation-Driven Development Foundation of Guangxi Province (Grant No. AA17204063), and the Research Council of Norway (Grant No. 243642). The authors acknowledge PRACE awarding access to resource Mare Nostrum based in Spain at BSC-CNS.

References

[1] M.A. Contreras, B. Egaas, K. Ramanathan, J. Hiltner, A. Swartzlander, F. Hasoon, R. Noufi, Prog. Photovoltaics Res. Appl. 7 (1999) 311–316.
[2] K. Ramanathan, M.A. Contreras, C.L. Perkins, S. Asher, F.S. Hasoon, J. Keane, D. Young, M. Romero, W. Metzger, R. Noufi, J. Ward, A. Duda, Prog. Photovoltaics Res. Appl. 11 (2003) 225–230.
[3] P. Jackson, R. Wuerz, D. Hariskos, E. Lotter, W. Witte, M. Powalla, Phys. Status Solidi-Rapid Res. Lett. 10 (2016) 583–586.
[4] W. Shockley, H.J. Queisser, J. Appl. Phys. 32 (1961) 510–519.
[5] A. Luque, A. Martí, Phys. Rev. Lett. 78 (1997) 5014–5017.
[6] R. Kudrawiec, A.V. Luce, M. Gladysiewicz, M. Ting, Y.J. Kuang, C.W. Tu, O.D. Dubon, K.M. Yu, W. Walukiewicz, Phys. Rev. Appl. 1 (2014) 034007.
[7] S. E. Jenks, Doctoral Thesis, Drexel University (2012).
[8] M. Dergal, H.I. Faraoun, A. Mahmoudi, Optik 135 (2017) 346–352.
[9] T. Wang, X. Li, W. Li, L. Huang, C. Ma, Y. Cheng, J. Cui, H. Luo, G. Zhong, C. Yang, Mater. Res. Express 3 (2016) 045905.
[10] B. Marsen, L. Steinkopf, A. Singh, H. Wilhelm, I. Lauermann, T. Unold, R. Scheer, H.W. Schock, Sol. Energy Mater. Sol. Cells 94 (2010) 1730–1733.
[11] J. Zhu, L. Xiao, T. Ding, Y. Wang, Y. Fan, J. Appl. Phys. 118 (2015) 115305.
[12] X. Lv, S. Yang, M. Li, H. Li, J. Yi, M. Wang, G. Niu, J. Zhong, Sol. Energy 103 (2014) 480–487.
[13] P. Chen, M. Qin, H. Chen, C. Yang, Y. Wang, F. Huang, Phys. Status Solidi A 210 (2013) 1098–1102.
[14] B. Marsen, S. Klemz, T. Unold, H.W. Schock, Prog. Photovoltaics Res. Appl. 20 (2012) 625–629.
[15] C. Yang, M. Qin, Y. Wang, D. Wan, F. Huang, J. Lin, Sci. Rep. 3 (2013) 1286.
[16] M.S. Qin, F.Q. Huang, P. Chen, Appl. Mech. Mater. 148 (2012) 1558–1561.
[17] C. Tablero, Thin Solid Films 519 (2010) 1435–1440.
[18] I. Aguilera, P. Palacios, P. Wahnón, Sol. Energ. Mat. Sol. Cells 94 (2010) 1903–1906.
[19] J. Hashemi, A. Akbari, S. Huotari, M. Hakala, Phys. Rev. B 90 (2014) 075154.
[20] M. Han, X. Zhang, Z. Zeng, RSC Adv. 4 (2014) 62380–62386.
[21] J. Koskelo, J. Hashemi, S. Huotari, M. Hakala, Phys. Rev. B 93 (2016) 165204.
[22] M. Han, X. Zhang, Y. Zhang, Z. Zeng, Sol. Energy Mater. Sol. Cells 144 (2016) 664–670.
[23] C. Tablero, D. Fuertes Marrón, J. Phys. Chem. C 114 (2010) 2756–2763.
[24] P. Palacios, I. Aguilera, P. Wahnón, J.C. Conesa, J. Phys. Chem. C 112 (2008) 9525–9529.
[25] C. Guo, C. Yang, Y. Xie, P. Chen, M. Qin, R. Huang, F. Huang, RSC Adv. 6 (2016) 40806–40810.
[26] D. Huang, J.W. Jiang, J. Guo, Y.J. Zhao, R. Chen, C. Persson, Semicond. Sci. Tech. 32 (2017) 065007.
[27] Y. Kumagai, Y. Soda, F. Oba, A. Seko, I. Tanaka, Phys. Rev. B 85 (2012) 033203.
[28] J.H. Boyle, B.E. McCandless, W.N. Shafarman, R.W. Birkmire, J. Appl. Phys. 115 (2014) 223504.
[29] J.J. Wu, C.Y. Yang, J.C. Sung, C.H. Lu, J. Am. Ceram. Soc. 98 (2015) 3911–3917.
[30] R.V. Forest, E. Eser, B.E. McCandless, J.G. Chen, R.W. Birkmire, J. Appl. Phys. 117 (2015) 115102.
[31] G. Kresse, J. Hafner, Phys. Rev. B 47 (1993) 558–561.
[32] G. Kresse, D. Joubert, Phys. Rev. B 59 (1999) 1758–1775.
[33] J. Heyd, J.E. Peralta, G.E. Scuseria, R.L. Martin, J. Chem. Phys. 123 (2005) 174101.
[34] H. Xiao, J. Tahir-Kheli, W.A. Goddard III, J. Phys. Chem. Lett. 2 (2011) 212–217.
[35] H.J. Monkhorst, J.D. Pack, Phys. Rev. B 13 (1976) 5188–5192.
[36] D. Huang, C. Persson, Chem. Phys. Lett. 591 (2014) 189–192.
[37] C. Ambrosch-Draxl, J.O. Sofo, Comput. Phys. Commun. 175 (2006) 1–14.
[38] Y. Zhang, L. Xi, Y. Wang, J. Zhang, P. Zhang, W. Zhang, Comp. Mater. Sci. 108 (2015) 239–249.
[39] D. Huang, C. Persson, Z. Ju, M. Dou, C. Yao, J. Guo, Europhys. Lett. 105 (2014) 37007.
[40] S. Maintz, V.L. Deringer, A.L. Tchougréeff, R. Dronskowski, J. Comput. Chem. 34 (2013) 2557–2567.
[41] R. Dronskowski, P.E. Bloechl, J. Phys. Chem. 97 (1993) 8617–8624.
[42] S. Kotochigova, Z.H. Levine, E.L. Shirley, M.D. Stiles, C.W. Clark, Phys. Rev. A 55 (1997) 191–199.
[43] Y. Gai, J. Li, S.S. Li, J.B. Xia, S.H. Wei, Phys. Rev. Lett. 102 (2009) 036402.